

**BLUE LUMINESCENT THIOPHENE BASED
C₃-SYMMETRIC STAR SHAPED DISCOTIC
LIQUID CRYSTAL**

By

Ishan Sarkar

A dissertation submitted in partial
fulfillment of the requirements for
the degree of

BS-MS dual integrated



**INDIAN INSTITUTE OF SCIENCE, EDUCATION AND
RESEARCH, MOHALI**

June 2020

CERTIFICATE OF EXAMINATION

This is to certify that the dissertation titled “Blue Luminescent Thiophene Based C_3 -Symmetric Star Shaped Discotic Liquid Crystal” submitted by Mr. Ishan Sarkar (Reg. No. MS15094) for the partial fulfilment of BS-MS dual degree program of the Institute, has been examined by the thesis committee duly appointed by the Institute. The committee finds the work done by the candidate satisfactory and recommends that the report be accepted.

Dr. Angshuman Roy Choudhury Dr. Raj Kumar Roy Dr. Santanu Kumar Pal

(Supervisor)

DECLARATION

The work presented in this dissertation has been carried out by me under the guidance of Dr. Santanu Kumar Pal at the Indian Institute of Science Education and Research Mohali. This work has not been submitted in part or in full for a degree, a diploma, or a fellowship to any other university or institute. Whenever contributions of others are involved, every effort is made to indicate this clearly, with due acknowledgement of collaborative research and discussions. This thesis is a bonafide record of original work done by me and all sources listed within have been detailed in the bibliography.

Ishan Sarkar

(Candidate)

Dated: June 4, 2020

In my capacity as the supervisor of the candidate's project work, I certify that the above statements by the candidate are true to the best of my knowledge.

Dr. Santanu Kumar Pal

(Supervisor)

ACKNOWLEDGEMENT

BS-MS dual degree program at IISER Mohali, it was an incredible and inspiring journey. I would like to thank several people for helping me through this course in various ways.

To commence with, I pay my obeisance to the Almighty to have bestowed upon me, good health, inspiration, courage, zeal and the light. I want to express my sincere gratitude to my advisor Dr. Santanu Kumar Pal, Associate Professor, Department of Chemical Science, Indian Institute of Science Education and Research, Mohali for the continuous support of my master's project. Besides my advisor, I would like to thank the rest of my thesis committee: Dr. Raj Kumar Roy and Dr. Angshuman Roy Choudhury for their encouragement, insightful comments, and hard questions.

I want to express my sincere gratitude to Mr. Joydip De for the continuous support of my master's project, for his patience, motivation, enthusiasm, and immense knowledge. His guidance helped me in all the time of research and writing of this thesis. I could not have imagined having a better mentor for my master's project.

I thank my fellow lab mates from Dr. Pal's research group, especially Indu Bala, Madhusudan Maity, Ritobrata De, Yogi and Shruti for the stimulating discussions, for all the fun we have had in the last fifteen months.

I thank my friends in IISER: Debanjan, Debjit, Nilangshu, Nikhil, Amit, Apoorv, Anubhav and all others who have been encouraging me in hard times and also have been parts of evening tea parties. Also, I thank all my seniors for being a role model and juniors for their cheerful support.

Last but not the least, I would like to thank my family, my parents Nilkanta Sarkar and Eti Sarkar for supporting me spiritually throughout my life.

Ishan Sarkar

LIST OF FIGURES

<i>Number</i>	<i>Page</i>
I.	Figure 1.1: (a) Crystal (3D lattice), (b) smectic LC phase (2D lattice), (c) nematic phase (orientation is present), (d) isotropic (no orientation).2
II.	Figure 1.2: Director and tilt angle in a mesophase.3
III.	Figure 1.3: Classification of liquid crystals.4
IV.	Figure 1.4: Molecular assemblies of liquid crystals showing different mesophases.4
V.	Figure 1.5: (i) Cyclohexane as the simplest core; (ii) hexabenzocoronene being one of the complex cores.6
VI.	Figure 1.6: (a) π -Stacking in a columnar assembly, (b) disc shaped molecules exhibiting nematic and columnar assembly, (c) columnar hexagonal packing, (d) columnar rectangular assembly.7
VII.	Figure 1.7: (a) Schematic representation of allowed electron flow through a columnar assembly, (b) working principle of OLEDs....8
VIII.	Scheme 1: Schematic representation of synthesizing TPN core.9
IX.	Scheme 2: Schematic representation of synthesizing 5-ethynyl-1,2,3-trialkoxybenzene.11
X.	Scheme 3: Schematic representation of synthesizing TPN derivatives.11
XI.	Figure 2.1: Working principle of polarizing optical microscopy..13
XII.	Figure 2.2: Polarizing optical micrographs of the samples (a) 6.1 at 25 °C (b) 6.2 at 25 °C (c) 6.3 at 25 °C on cooling the isotropic melts to room temperature.14
XIII.	Figure 2.3: Schematic representation of the working principle of DSC.15
XIV.	Figure 2.4: Thermograms obtained DSC studies (a) 6.1 , (b) 6.2 and (c) 6.3 ; all the cycles were measured at an interval of 10 °C/min. .16
XV.	Figure 2.5: TGA curves of (a) 6.1 , (b) 6.2 and (c) 6.3 . The measurements were performed under a nitrogen atmosphere, with heating and cooling rates of 10 °C/min.17
XVI.	Figure 2.6: Small angle and wide angle (inset) X-ray diffraction pattern of compound (a) 6.1 , (b) 6.2 and (c) 6.3 at 25 °C.....19

XVII.	Figure 2.7: Photoluminescence spectra of the compounds 6.1-6.3 ; (a)-(d) emission and excitation spectra of 6.1 ; (b)-(e) emission and excitation spectra of 6.2 ; (c)-(f) emission and excitation spectra of 6.3	22
XVIII.	Figure 2.8: Cyclic voltammograms of (a) 6.1 , (b) 6.2 and (c) 6.3 in HPLC DCM solution of TBAP (0.1 M) at a scanning rate 50 mVs ⁻¹	24
XIX.	Figure 2.9: (a) Diagram of energy-level of emitter 6.1 used with (CBP) host for fabrication of the device. (b) luminance-voltage, (c) Current density-voltage, (d) current efficiency-luminance, (e) power efficiency-luminance and (f) electroluminescence plots of the solution-processed OLED devices using CBP host with 1, 3, 5 and 100 wt% 6.1 dopant concentrations. Inset of (f) shows EL emission of the OLED device	25

LIST OF TABLES

I.	Table 2.1: Summarized data of phase transitions of 6.1-6.3	16
II.	Table 2.2: The observed and calculated d-spacings & planes of the diffraction peaks of 6.1 in oblique lattice observed at 25 °C.....	19
III.	Table 2.3: The observed and calculated d-spacings & planes of the diffraction peaks of 6.2 in oblique lattice observed at 25 °C.....	20
IV.	Table 2.4: The observed and calculated d-spacings & planes of the diffraction peaks of 6.3 in oblique lattice observed at 25 °C.....	20
V.	Table 2.5: Summary of photoluminescence Data.....	23
VI.	Table 2.6: Comparing band gap from UV-Vis and CV	24
VII.	Table 2.7: Effect of doping concentration on the power efficiency (PE), current efficiency (CE), external quantum efficiency (EQE), CIE coordinates, and maximum luminance of solution-processed OLED devices with the CBP host for 6.1	26

TABLE OF CONTENTS

Certificate of Examination	i
Declaration.....	iii
Acknowledgment	v
List of Figures	vii
List of Tables	ix
Table of Contents	xi
Abstract.....	xiii
Chapter 1: Introduction	1
1.1 States of Matter	1
1.2 To Liquid Crystals	2
1.2.1 Order Parameter	3
1.3 Types of Liquid Crystals.....	3
1.4 Thermotropic Liquid Crystal	5
1.5 Discotic Liquid Crystal	5
1.6 Organic Electronics.....	7
Chapter 2: Characterization Techniques and Apparatus Involved	9
2.1 Introduction	9
2.2 Experimental Procedure.....	9
2.2.1 Synthesis of 1,3,5-Tri(2'-thienyl)benzene.....	10
2.2.2 Synthesis of 1,3,5-Tri(5'-bromo-2'-thienyl)benzene.....	10
2.2.3 Synthesis of Mesogens	10

2.2.4 Synthesis of TPN derivatives	11
2.3 Thermal Analysis	22
2.3.1 Polarizing Optical Microscopy Studies.....	13
2.3.2 Differential Scanning Calorimetric Studies	14
2.3.3 Thermo-gravimetric Analysis.....	16
2.3.4 X-ray Diffraction Studies	17
2.4 Photo physical Studies	20
2.4.1 Absorption and Emission Studies.....	20
2.4.2 Electrochemical Studies.....	23
2.4.3 OLED Fabrication.....	25
Chapter 3: Conclusion and Further Outlook	27
Appendices: NMR data of compounds 6.1-6.3	29
Bibliography	37

ABSTRACT

Organic electronics is a relatively new branch of modern electronics and has immensely advantageous against inorganic electronics. Unlike them, organic electronics have comparatively low cost of production, high flexibility, high tunability and many more. One of the main fields emerging from this topic is Organic Light Emitting Diodes (OLEDs) and especially blue luminescence is one of the features which are pretty challenging and a very active research field within the topic itself. This thesis work was done in order to achieve blue luminescent discotic liquid. We used thiophene based discotic liquid crystals in order to achieve this very property since thiophene derivatives upon tweaking can show luminescence over a wide range of spectrum. We synthesized three different molecules of thiophene based benzene derivatives which show inconsistency only in the chain lengths at the periphery.

The aim of the first chapter is to introduce readers to the basics of Liquid Crystals and primarily address Discotic Liquid Crystals (DLCs).

The second chapter addresses the instrumentation techniques and summarizes the theories associated with it.

Chapter three of the thesis deals with the synthesis and characterization of the derivatives. The details of the experimental procedures have been added, and spectral, thermal, photo-physical, electrochemical behavior has been analyzed. The results shown in this chapter confirms the blue luminescent behavior of the compounds synthesized along with its DLC properties.

The final part of the thesis consists of the conclusions, future outlook and appendices.

Chapter 1

INTRODUCTION

1.1 State of Matter:

A state of matter scientifically suggests one distinct form in which a matter or material can exist in nature. Solid, liquid and gas are the three states commonly encountered in daily life (plasma being considered as the fourth one). But for some special substances, an intermediate state can also be found which has properties between the liquids and solid crystals.

A solid is a state of matter where the atoms or the molecules of the substance is very closely bound to each other by very strong intermolecular forces, so great that the molecules cannot leave the closely packed system i.e. lattice. This also implies that the molecules has the least amount of kinetic energy available amongst all the other states. If the translational and rotational degrees of freedoms are concerned, then all six of them (translation along three axes and rotation in three planes) are restricted in a solid except for plastic crystals where rotation of molecules which forms the lattice doesn't break the symmetry of the lattice.

Liquid is the state of matter in which a substance shows fluidic behavior but occupies a nearly fixed volume which essentially means it's almost incompressible, although some adiabatic changes can compress some liquids to a considerable amount. In case of liquids, all six of the translational and rotational degrees are allowed, i.e. they are irregularly oriented (Isotropic). This is actually a consequence of increased temperature environment than its solid form which cancels out most of the strong intermolecular forces.¹

When the constituents of a substance are fairly distant from each other, resulting in the negligible amount of interaction in between molecules is declared as a gaseous phase.

1.2 To Liquid Crystals:

As the name suggests, liquid crystals bear properties of two different phases and appears as an intermediate phase between isotropic liquid and crystalline solid. It possesses definite amount of viscosity which is a critical property of fluids and shows anisotropy which a characteristic of crystals. These types of in-between phases are termed as “mesophase”.²

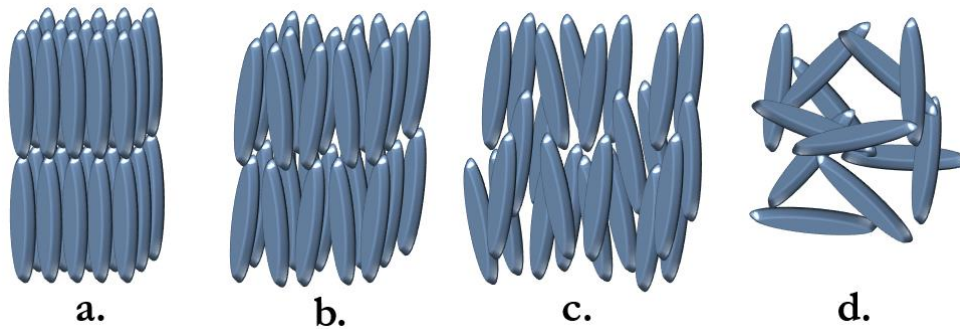


Figure 1.1: (a) Crystal (3D lattice), (b) smectic LC phase (2D lattice), (c) nematic Phase (orientation is present), (d) isotropic (no orientation).

In solid crystals three dimensional ordering (rotational and translational) whereas traditional liquids have no ordering at all. However, liquid crystals does have somewhat ordering in a long range but not all of the degrees of freedom can be found at the same time. Depending on the degrees present, liquid crystals have different sub phases.

The liquid crystal molecules tend to show an average alignment towards a particular direction or axis called ‘director’ and denoted as ‘n’. The molecular axis may or may not align with the director ‘n’ but will always be at an angle ‘ Θ ’ and the value of this angle cannot exceed 90° .

1.2.1 Order Parameter

The theoretical analysis of liquid crystals in terms of entropy and free energy in order to predict different phase transitions gives rise to a quantity called order parameter, usually depicted as ‘S’. This order parameter is actually an average value of the second Legendre polynomial which comes from the Rodrigues’ formula.

$$S = \langle P_2(\cos\theta) \rangle = \left\langle \frac{3\cos^2\theta - 1}{2} \right\rangle$$

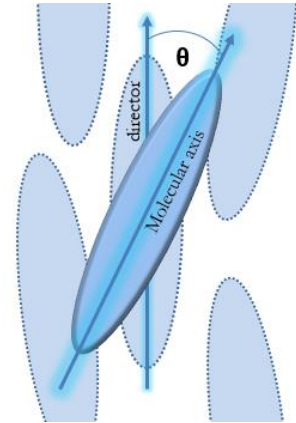


Figure 1.2: Director and tilt angle.

The angle Θ is the director-molecular axis angle as mentioned above. From the formula itself, it can be understood that S can obtain all the values possible from 0 to 1. For a perfectly ordered crystal, $S=1$ and isotropic liquid, $S=0$; and Θ being all the possible distribution in between 0 to 90, it can be written that $0 < S < 1$ for liquid crystals.

1.3 Types of Liquid Crystals:

Liquid crystals can be classified on the basis of their molecular weight/mass, such as higher molecular weight and lower molecular weight. They can also be divided in further class as described in **Figure 1.3**. Liquid crystal is phase and can be achieved not only in molecules but also in a composite systems such as binary or ternary mixtures. Depending on that liquid crystals can be classified as thermotropic liquid crystals and lyotropic liquid crystals. As the name suggests, thermotropic LC phases are achieved by perturbing temperature.^{3,4}

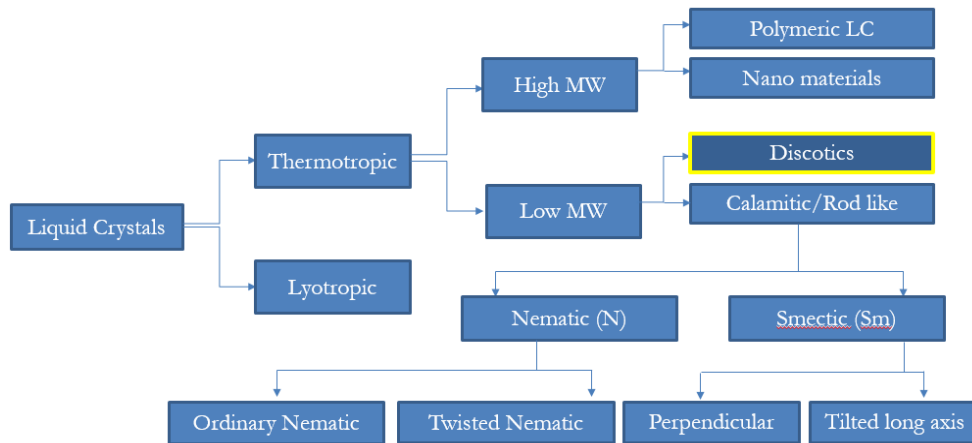


Figure 1.3: Classification of liquid crystals.

The term “lyotropic” essentially means water mixtures i.e. apart from using temperature to achieve liquid crystal phase, varying concentration can also lead to the same goal. This essentially means that lyotropic LCs are composites. In the solid crystals water molecules are added in such a concentration that it perturbs the lattice just a bit to make it mobile. More addition makes it a solution. Sometimes addition of solvent to a powder of a substance enhances nano-structure formation which shows liquid crystalline behavior as shown in some chromonic LCs.

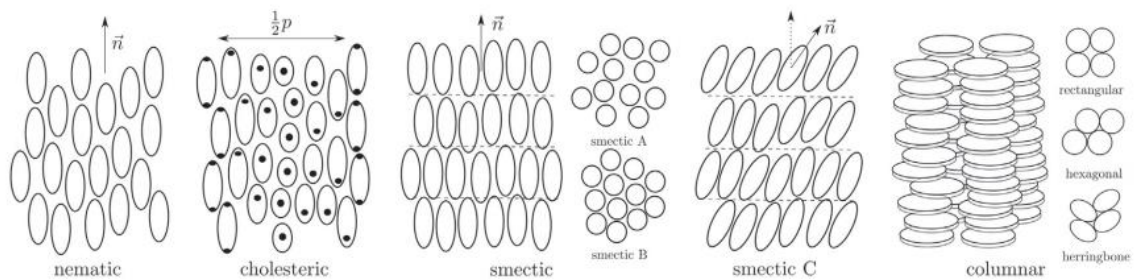


Figure 1.4: Molecular assemblies of liquid crystals showing different mesophases. (Adapted from Ref. 5).

Liquid crystals can also be subdivided based on the shapes of its core, e.g. rod like calamitic, disc shaped discotic and banana shaped bent-core.

1.4 Thermotropic Liquid Crystals

As the name suggests, thermotropic means changes when heat is involved. When temperature is increased, the crystal structure loses its degrees of freedom one by one and upon losing all of them, it becomes a liquid which is in scientific terms, called isotropic. Needless to say that the difference in the degrees of freedom gives rise to different sub phases. The more the degrees, the closer it is to the crystal phase.

To attain a thermotropic behavior, a compound must possess some necessary characteristics. The compound has to have a rigid core e.g. aromatic cores, biological structures which have specific structures and doesn't alter such as cholesterols.⁶ Depending on the shape of the core, thermotropic LCs can be divided into three main subclasses i.e. rod like, discotic and bent-core. The main characteristics which gives the property of a liquid crystal is the flexible alkyl chains which are meant to be attached to/around the rigid core. More numbers of chains and the length of the chains have a huge impact on the temperature boundaries of the respective Liquid crystal. Longer the chain, less is isotropic to liquid crystal (nematic) transition temperature. Chirality in the chains or in the core also induces different opto-mechanical properties.

Since my work is mostly on the disc shaped columnar mesogens, it is highly necessary to introduce the readers with the discotic liquid crystals.

1.5 Discotic Liquid Crystals

As mentioned earlier, DLCs have a rigid core which are generally aromatic in nature which has at least six long aliphatic chains attached with itself. This attachment can be direct or can be via different linking groups such as ether, ester or alkyne linkages. Even if the core is not planar, it is very important to minimize the overall height of the disc, which if not maintained, can prevent effective packing in between molecules, i.e. prevents columnar phase formation. More than 50 different cores are reported in the literature.⁷

Cyclohexane as a DLC core shows us that puckering in the central core, can lead to a good packing, enough to show us columnar packing. However, hexabenzocoronene shows us good π -stacking can also lead us to columnar packing.⁸

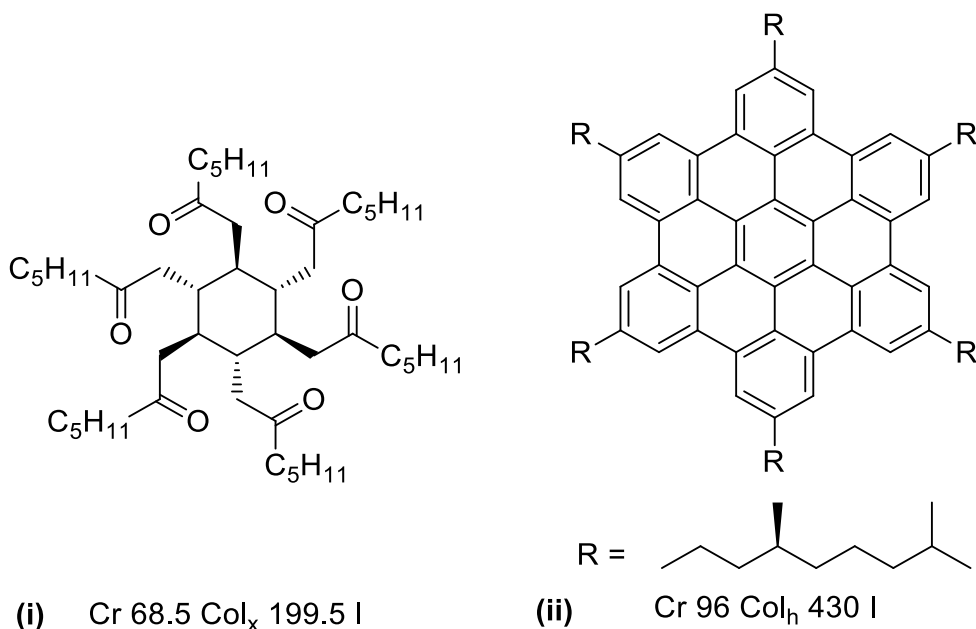


Figure 1.5: (i) Cyclohexane as the simplest core; (ii) hexabenzocoronene being one of the complex cores.

DLC shows mainly discotic nematic phase and columnar discotic phase (common) which has several sub phases.^{9, 10}In nematic discotic phase, the stacking does not play any role whatsoever. In Columnar phase, the stacking makes a column, and depending on the way the columns are aggregated, it can have hexagonal, rectangular etc. arrangements which can be understood from the **Figure 1.6** given below.

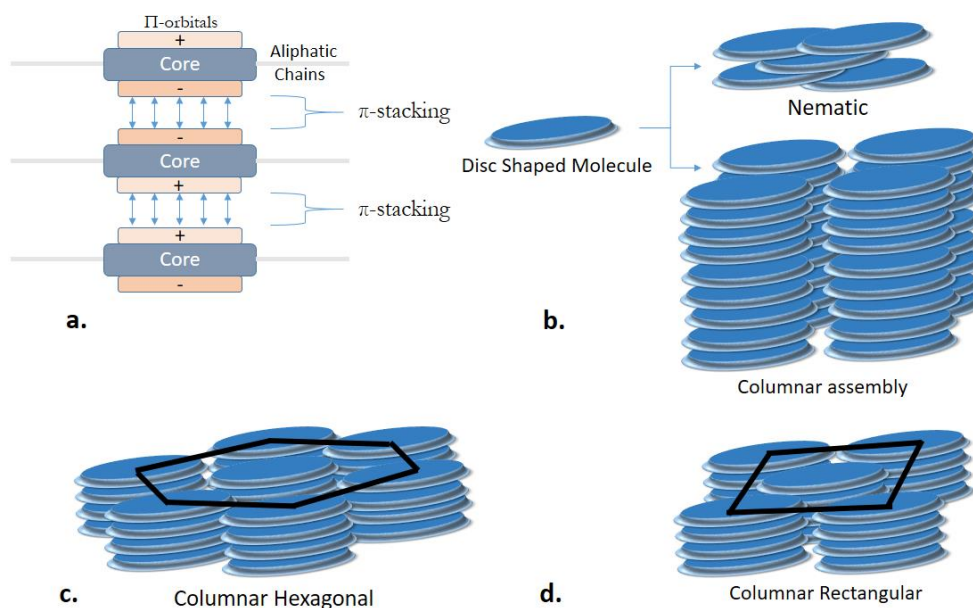


Figure 1.6: (a) π -Stacking in a columnar assembly, (b) disc shaped molecules exhibiting nematic and columnar assembly, (c) columnar hexagonal packing, (d) columnar rectangular assembly. (Redrawn from Ref. 11).

Columnar mesophases also have different other Assemblies such as oblique assemblies, helical assemblies generated in chiral molecules and plastic phases can also be sub phases of the previous phases. Although hexagonal assembly is relatively general, rectangular phase requires more recognition to specific sites which helps them to pack efficiently.¹²

1.6 Organic Electronics

Organic electronics is a relatively new field of technology which deals with synthesis, characterization and application of organic molecules which show desirable electronic conductivity. In comparison to traditional inorganic electronic, it has promisingly low cost to synthesize and fabricate and promisingly high flexibility. Some of them are highly stable even on high temperatures.¹³

Conductive Polymers are one of the branches where polymers having long pi-network is generally used which makes it intrinsically conductive. The structures of the compounds can be tweaked to have desirable conductivity and some can be modified to show even electroluminescence.¹⁴

Organic Light Emitting Diodes (OLEDs) are another class of organic electronics where the difference in HOMO-LUMO band gap in the same compound can be exploited in order to emit light as energy. Fluorescent and phosphorescent compounds are very commonly used since the band gap of the compounds are well within reach and can be excited while expending very low energy.¹⁵

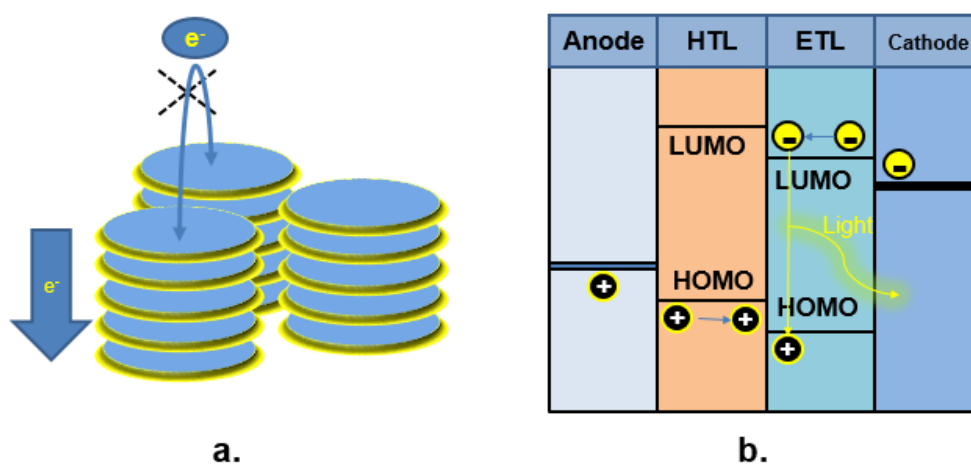


Figure 1.7: (a) Schematic representation of allowed electron flow through a columnar assembly, (b) working principle of OLEDs.

Organic field-effect transistors (OFET) uses organic molecules as conducting or semiconducting material. A field-effect transistor behaves as if a capacitor is attached to a conducting channel in between a source and a sink electrode. Voltage applied on the gate electrodes control how many charge carriers should be flowing through the system.¹⁶

The goal of this project is to build a molecule that shows DLC properties as well as a suitable band gap to show blue luminescence suitable for OLED fabrication.

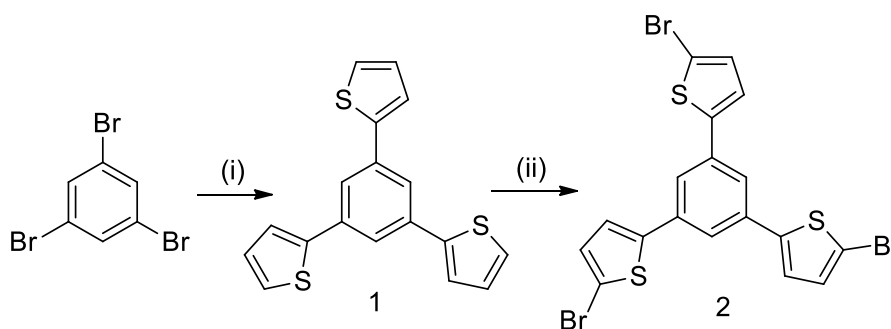
RESULTS AND DISCUSSIONS

2.1 Introduction

To be able to apply as a material which can show properties such as aggregation induced emission (AIE), the material has to have a chromophore as the core of the discotic liquid crystal. Although there are more than fifty different cores reported having different luminescent properties out of which blue luminescent ones are highly of interest and reported very few in numbers. There are countless research articles showing that the thiophene moieties can be tweaked in order to achieve the desired luminescence.¹⁷ This motivated us to synthesize DLCs based on thiophene and we came up with 1,3,5-Tri(5'-bromo-2'-thieneyl)benzene (TPN) as our core. To give it the properties of DLCs, mesogens are attached to the thiophene moieties via alkyne linkage.

2.2 Experimental Procedure

The synthesis scheme is described in details in the following scheme given below. The first step is a text book reaction commonly known as Stille coupling.¹⁸ The reaction following is just a bromination approach by N-bromosuccinimide.



Scheme 1: Schematic representation of synthesizing TPN core. Reagents used: (i) 2-(tributylstannyl)thiophene, Pd(PPh₃)₂Cl₂, dry DMF; (ii) NBS, TMS-Cl, CH₃CN, r.t, 2 h.

2.2.1 Synthesis of 1,3,5-Tri(2'-thieneyl)benzene

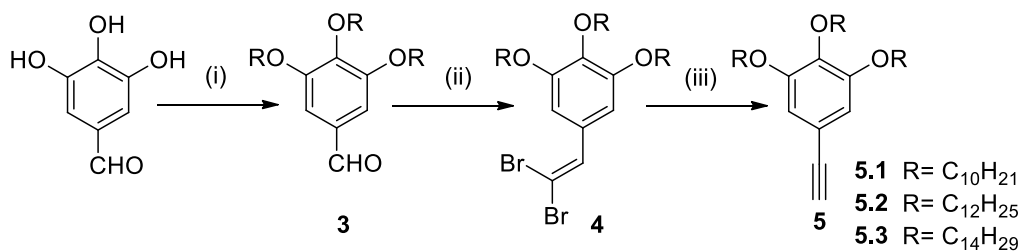
2-(Tributylstannyl)thiophene (6.06 ml, 19.0597 mmol) was poured into a solution made up of 1,3,5-tribromobenzene (1.5 g, 4.765 mmol) and Pd(PPh₃)₂Cl₂ (237.804 mg, 0.3388 mmol) in anhydrous DMF kept in nitrogen atmosphere maintained inside a 100ml RB flask. The temperature of the resulting mixture was increased to 100 °C at least for 16 hrs. After cooling the mixture down to room temperature, extraction was performed using ether and water. The organic solution thus collected, was dehydrated over anhydrous Na₂SO₄ and amassed using a rotary evaporator. The mixture was then purified by column chromatography (ethyl Acetate: hexane 0.6:99.4) and obtained the product (yield 54.33%) as beige solid. Proton NMR (¹H, 400 MHz, CDCl₃, δ ppm): 7.77 (s, 3H), 7.45 (d, *J* = 3.56 Hz, 3H), 7.38 (d, *J* = 5.08 Hz, 3H), 7.16 (t, *J* = 4.68 Hz, 3H).

2.2.2 Synthesis of 1,3,5-Tri(5'-bromo-2'-thieneyl)benzene

In complete deprivation of light, **1** (430.5 mg, 1.3267 mmol) was poured into a mixture of NBS (630.48 mg, 3.5424 mmol) in dry CH₃CN (25 ml) kept in a 100 ml two necked RB, where slight TMSCl (0.1 ml) driblets were put in to initiate the reaction. This entire setup was kept in room temperature and constant stirring was done for 2 hrs.¹⁹ CH₃CN was gotten rid of using rotary evaporator and the organic solution remaining was treated with DCM/water in order to carry out extraction several times and was dehydrated over anhydrous sodium sulphate. The mixture was then filtered out using column chromatography in (EtOAc: hexane = 0.3: 99.7) and **2** was procured (yield 67.13%) as a beige colored solid. NMR (¹H, 400 MHz, CDCl₃, δ ppm): 7.54 (s, 3H), 7.15 (d, *J* = 3.84 Hz, 3H), 7.10 (d, *J* = 3.88 Hz, 3H).

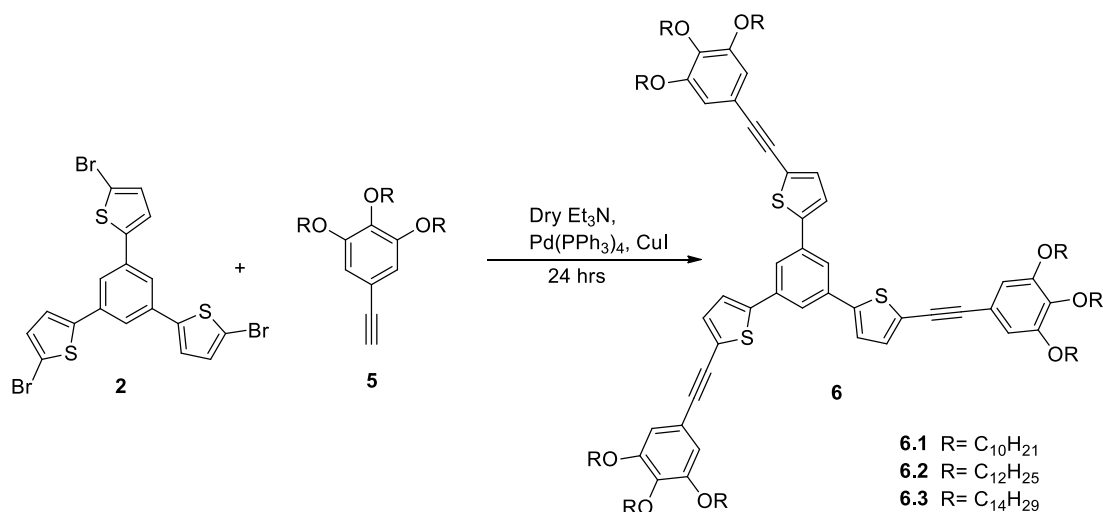
2.2.3 Synthesis of the Mesogens

Synthesis of the mesogen 5-ethynyl-1,2,3-trialkoxybenzene was done as the following schematic diagram represents. First step involves alkylation process in slightly basic medium. The following is a Corey-Fuchs reaction which ends up giving us 5-ethynyl-1,2,3-trialkoxybenzene. In order to get different derivatives, the carbon chains used in the first step was varied as 10C, 12C and 14C.²⁰



Scheme 2: Schematic representation of synthesizing 5-ethynyl-1,2,3-trialkoxybenzene. Reagents used: (i) R-Br, K₂CO₃, dry DMF, KI, 90-95 °C, 20 hrs; (ii) CBr₄, PPh₃, DCM (dry), 0-5 °C, 20-25 mins; (iii) n-butyl lithium, dry THF, r.t., 48 h.

2.2.4 Synthesis of TPN derivatives



Scheme 3: Schematic representation of synthesizing TPN derivatives.

Synthesis of 1,3,5-tris(5-((3,4,5-tris(decyloxy)phenyl)ethynyl)thiophen-2-yl)benzene

45 ml of dry triethylamine and 15 ml of dry DMF was taken into a 100ml two necked RB and nitrogen gas was purged into it for 10-15 mins, compound **2** (305.79 mg, 0.545 mmol) was dissolved into the mixture by applying slight heating. Then Pd(PPh₃)₄ (48.534 mg, 0.077 mmol), CuI (9.35 mg, 0.049 mmol), **5.1** (1.4 g, 2.452 mmol) were added respectively. Then the temperature of the mixture was increased up to 90 °C, left for reflux for 24 hrs.^{21,22} Upon completion, the setup was brought back to room temperature and the solvent was gotten rid of in a rotary evaporator. The mixture left was extracted using diethyl ether/water, dehydrated

over anhydrous Na_2SO_4 and purification was performed using column chromatography (neutral alumina, ethyl acetate: hexane- 4.5: 95.5) and yellow colored product **6.1** was obtained (yield 36.15%). ^1H NMR (400 MHz, methylene chloride- d_2 , δ ppm): 7.78 (s, 3H), 7.42 (d, $J = 3.72$ Hz, 3H), 7.34 (d, $J = 3.88$ Hz, 3H), 6.78 (s, 6H), 4.04-3.99 (m, 18H), 1.87-1.74 (m, 18H), 1.58-1.30 (m, 18H), 1.21-1.17 (m, 126H), 0.93-0.89 (m, 27H). ^{13}C (100MHz, chloroform- d , δ ppm): 153.06, 144.14, 139.31, 135.33, 132.83, 124.02, 123.60, 122.69, 117.07, 109.88, 94.82, 81.35, 73.59, 69.14, 31.98, 31.95, 30.34, 29.78, 29.72, 29.68, 29.63, 29.43, 29.40, 29.34, 26.11, 22.73, 14.16.

Synthesis of 1,3,5-tris(5-((3,4,5-tris(dodecyloxy)phenyl)ethynyl)thiophen-2-yl)benzene

Compound **6.2** was obtained by following the process similar to **6.1** which required **2** (182.94 mg, 0.326 mmol), $\text{Pd}(\text{PPh}_3)_4$ (22.65 mg, 0.0196 mmol), CuI (5.588 mg, 0.0293 mmol), **5.2** (961.046 mg, 1.467 mmol); yield = 33.15%. ^1H NMR (400 MHz, methylene chloride- d_2 , δ ppm): 7.78 (s, 3H),), 7.42 (d, $J = 3.8$ Hz, 3H), 7.34 (d, $J = 3.8$ Hz, 3H), 6.79 (s, 6H), 4.03-3.98 (m, 18H), 1.88-1.74 (m, 18H), 1.52-1.49 (m, 18H), 1.31 (m, 162H), 0.93-0.90 (m, 27H). ^{13}C (100MHz, chloroform- d , δ ppm): 153.05, 144.12, 139.33, 135.33, 132.81, 124.01, 123.60, 122.70, 117.06, 112.73, 109.90, 94.81, 81.34, 73.59, 69.15, 60.83, 31.95, 30.34, 29.78, 29.73, 29.67, 29.62, 29.43, 29.40, 29.34, 26.11, 22.72, 18.08, 14.15.

Synthesis of 1,3,5-tris(5-((3,4,5-tris(tetradecyloxy)phenyl)ethynyl)thiophen-2-yl)benzene

Compound **6.3** was obtained by following the process similar to **6.1** which required **2** (236.17 mg, 0.421 mmol), $\text{Pd}(\text{PPh}_3)_4$ (37.452 mg, 0.0324 mmol), CuI (7.218 mg, 0.0379 mmol), **5.3** (1.4 g, 1.894 mmol), yield = 37.47%. ^1H NMR (400 MHz, methylene chloride- d_2 , δ ppm): 7.78 (s, 3H),), 7.42 (d, $J = 3.76$ Hz, 3H), 7.34 (d, $J = 3.84$ Hz, 3H), 6.78 (s, 6H), 4.03-3.98 (m, 18H), 1.88-1.72 (m, 18H), 1.58-1.50 (m, 18H), 1.31 (m, 198H), 0.93-0.91 (m, 27H). ^{13}C (100MHz, chloroform- d , δ ppm): 153.07, 147.91, 144.14, 139.42, 139.34, 137.64, 135.34, 134.28, 132.82, 130.62, 124.02, 123.61, 123.14, 122.70, 119.89, 117.07, 111.51, 109.91, 102.37, 94.81, 82.37, 81.34, 73.59, 69.16, 64.58, 31.96, 30.34, 29.78, 29.74, 29.70, 29.68, 29.63, 29.43, 29.35, 27.83, 26.12, 22.73, 14.16.

2.3 Thermal Analysis

2.3.1 Polarizing Optical Microscopy Studies

Polarizing optical microscopy operates in a unique manner where two crossed polarizers are used and the sample has to be put in between the crossed polarizer. The mesophases show different textures under this setup and can be identified.

Liquid crystalline materials are optically anisotropic, which means that it has different optical properties (e.g. refractive index) depending on the position of the observation made. Now in the microscope, the light source used is unpolarized. When it passes through the first filter, it becomes linearly polarized. Another linear polarizer is placed in such a way that the axis of polarization is perpendicular to the previous one. Hence, in absence of any sample, the output should be black (**Figure 2.1**) i.e. no light should come out from the eye-piece.²³

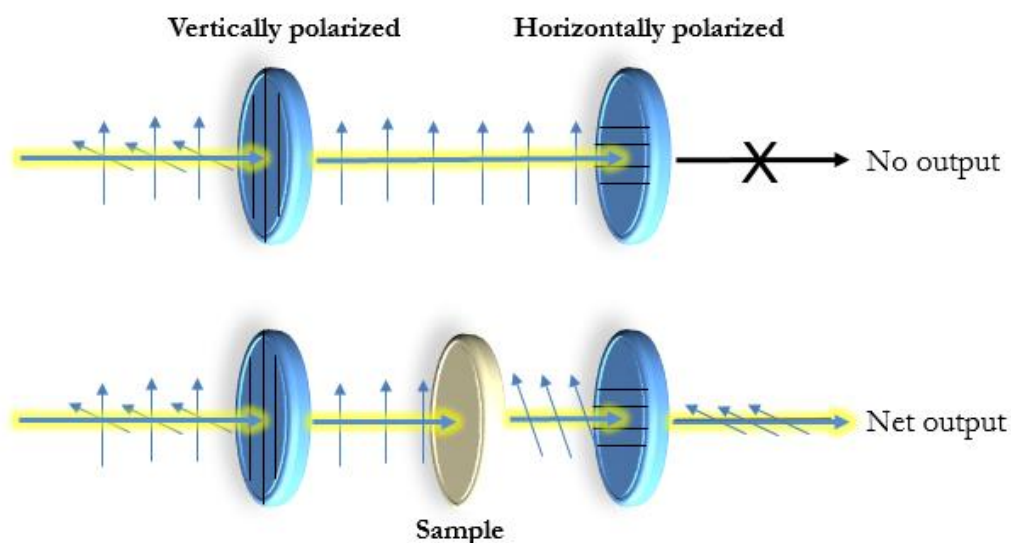


Figure 2.1: Working principle of polarizing optical microscopy.

When the sample is placed in between the cross-polarizers, the polarized light from the first filter has to pass through the sample and when it does, two different light of different polarization emerges out from the sample, one having the same polarization as the light from

the first which gets blocked by the second filter which has polarizing axis perpendicular to it. However, the other light i.e. extraordinary light has slightly tweaked polarization that allows it to pass through the second filter. That is the origin of textures which is different for different phases of the same compound, but has similarity in the same phase of different molecules.

The sample shows slight movement when pressure or stress is exerted on the sample which makes it different from crystals. All the samples were mounted as thin films produced by putting the samples into the customized cell of a clean glass slide and a clean cover slip in which all of them show sickle shaped textures (**Figure 2.2**) on cooling the isotropic melt to room temperature which confirms that the assemblies formed by the samples **6.1-6.3** are essentially columnar in nature.

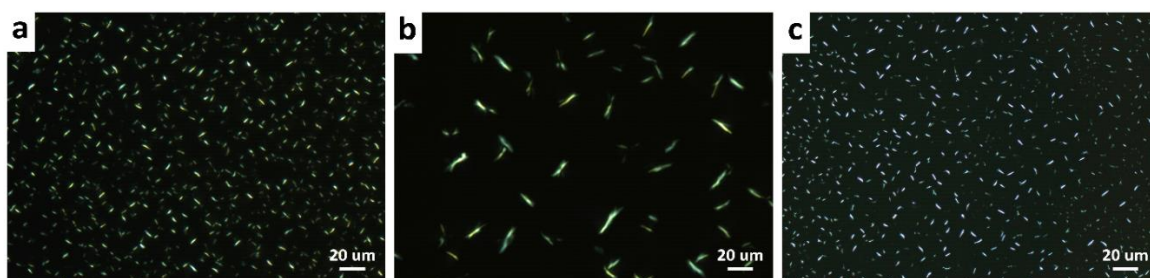


Figure 2.2: Polarizing optical micrographs of the samples (a) **6.1** at 25 °C (b) **6.2** at 25 °C (c) **6.3** at 25 °C on cooling the isotropic melts to room temperature.

2.3.2 Differential Scanning Calorimetric Studies

As the name suggests, this technique is a calorimetric process which essentially implies that measurement of heat change is involved. When a material changes the phase, extra energy is required/released in order to break/forming the intermolecular bonds or interaction. This calorimetric process works on the principle mentioned earlier and detects the abrupt heat change which corresponds to the extra heat change.²⁴

DSC experiment gives out a curve of heat flux versus the temperature change. When the sample goes from a ordered structure to a lower ordered structure, it takes some extra energy

(endothermic process) to break the intermolecular interactions and that's why a crest is observed in the curve; whenever there is a transition from a disordered structure to an ordered one, a trough is observed in the curve as it releases some energy (exothermic process).

In the apparatus itself, the sample is measured against a reference (**Figure 2.3**) where a continuous heat flux is maintained. The goal of the instrument is to measure the heat absorbed/released by the sample while keeping both the sample and reference at sample temperature which is done for a large spectrum of temperature.

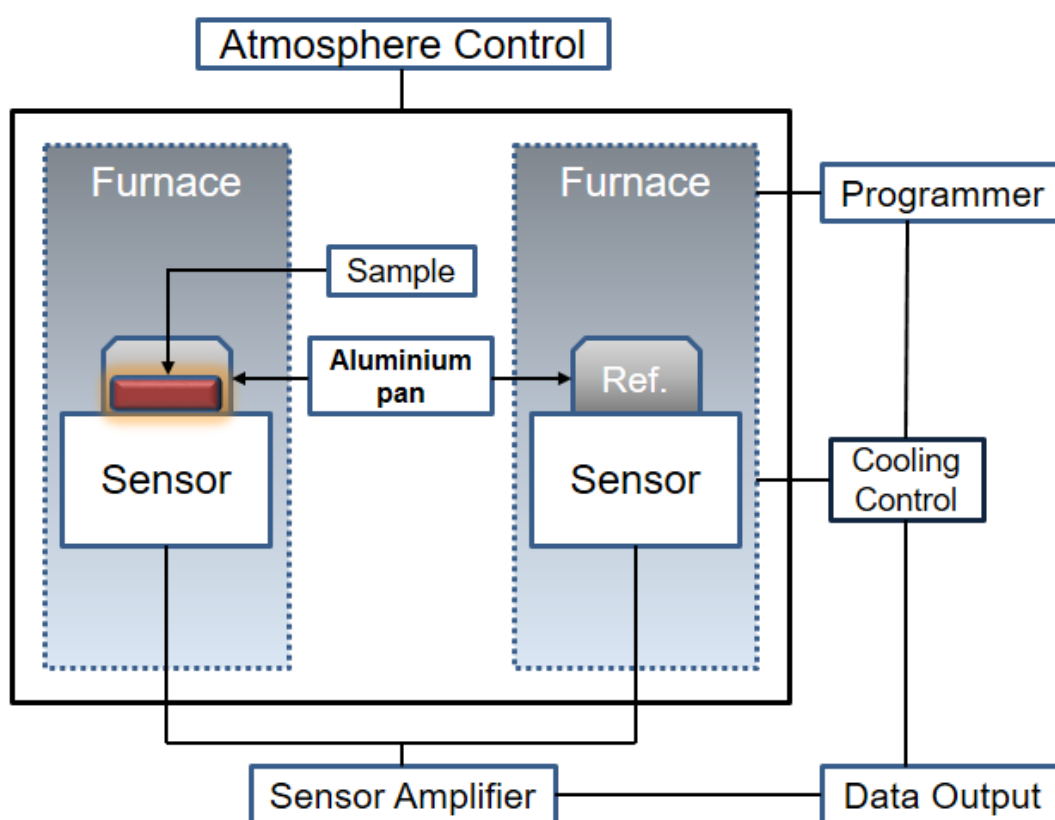


Figure 2.3: Schematic representation of the working principle of DSC.

DSC studies were performed on the samples (6.1-6.3) to pinpoint the transition temperature and the enthalpy exchanged during the process. From mesophase the transition occurs to give rise to the isotropic phase on the heating cycle and this happens at temperatures 81.1 °C, 82.8 °C and 77.5 °C for the samples 6.1-6.3 respectively. The reverse transformation

occurs on cooling the isotropic melt at temperatures **69.7 °C**, **72.5 °C** and **68.9 °C** for the samples **6.1-6.3** as described in the **Figure 2.4** and **Table 2.1**.

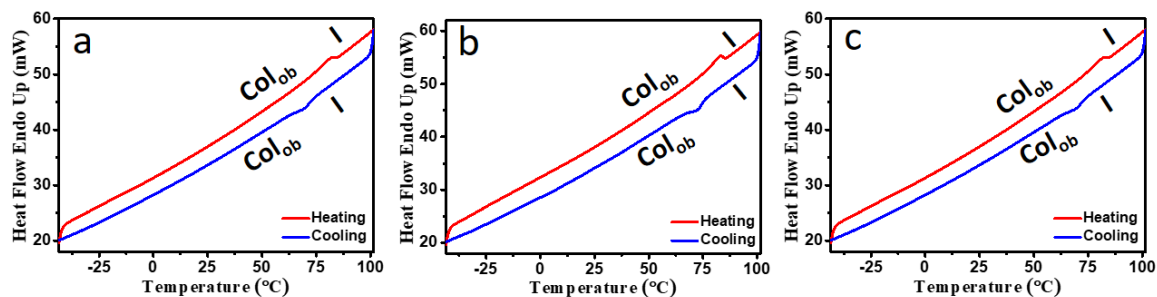


Figure 2.4: Thermograms obtained from DSC studies (a) **6.1**, (b) **6.2** and (c) **6.3**; all the cycles were measured at an interval of 10 °C/min (Abbreviations used: Col_{ob} = columnar oblique; I = isotropic).

TABLE 2.1: Summarized data of phase transitions of **6.1-6.3**

Compounds	On Heating	On Cooling
6.1	Col _{ob} 81.1 Iso	Iso 69.7 Col _{ob}
6.2	Col _{ob} 82.8 Iso	Iso 72.5 Col _{ob}
6.3	Col _{ob} 77.5 Iso	Iso 68.9 Col _{ob}

^a The temperature shown in the table is given in °C. ^b Abbreviations used: Col_{ob}= columnar oblique; Iso= Isotropic.

2.3.3 Thermo-gravimetric Analysis (TGA)

TGA analysis was carried out on the samples **6.1-6.3** in order to check stability under exposure to high temperatures. Compound **6.2** was recorded as the most stable among all three samples with 5% weight loss at **345 °C** and **6.1** was the least stable one with 5% weight loss recorded at **328 °C**. Compound **6.3** was recorded to have 5% weight loss at temperature **334 °C** (**Figure 2.5**).

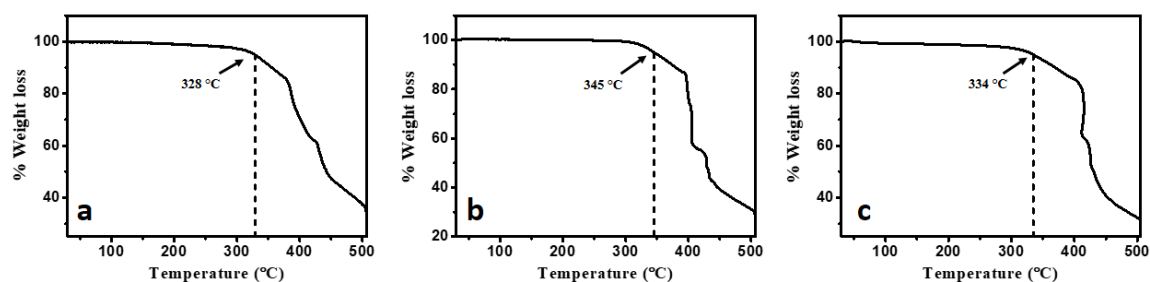


Figure 2.5: TGA plots of (a) **6.1**, (b) **6.2** and (c) **6.3**. The experiments were carried out under an inert nitrogen atmosphere, with heating and cooling rates of 10 °C/min.

2.3.4 X-ray diffraction Studies:

Crystals are a three dimensional network of atoms or molecules where they are specific distances apart from each other. However, it simply implies that the 3D lattice is basically a large number of planes are apart to each other by a specific distance which constant to that material. This applies to the liquid crystalline materials as well since they do have a long range ordering.²⁵ Now, the reflection of x-ray can occur from the molecules in each plane and the reflections from two adjacent planes, in order to a constructive interference, has to follow the rule which is

$$2d_{hkl}\sin\theta = n\lambda$$

This law is also known as Bragg's law where, d is the distance between planes described by the Miller indices h, k and l.²⁶ θ is the angle of incidence, λ is the wavelength of the x-ray used and n is any possible integer. The distance in between the layers can thus be found if other constraints are known. These spacing helps us to find the nature of the assemblies and the phases and gives oneself valuable information on lattice parameters, crystallinity, size and shape, necessary for characterization of liquid crystals.²⁷

The small angle x-ray scattering (SAXS) and wide angle x-ray scattering (WAXS) experiments has been performed to deduce the detailed structure of the assembly of compound **6.1**, **6.2** and **6.3**. The x-ray diffraction pattern of compound **6.1** in the mesophase

temperature range exhibits four peaks in small angle region. These peaks could be indexed on two dimensional oblique lattice. The d-spacings are calculated by using the relation $\frac{1}{d_c^2} = \frac{1}{(\sin\alpha)^2} \left[\frac{h^2}{a^2} + \frac{k^2}{b^2} - \frac{2 h k \cos\alpha}{ab} \right]$ where d_c is calculated d-spacing, a , b and angle α are the lattice parameters of the oblique lattice.

The calculated lattice parameters at temperature 25 °C at are found to be $a = 34.35 \text{ \AA}$, $b = 28.25 \text{ \AA}$ and $\alpha = 78.19^\circ$ (**Figure 2.6a, Table 2.2**). Moreover, there is one broad peak, h_a , in wide angle region of spacing 4.84 Å, appears due to fluid alkyl chain-chain correlation. And there is also one broad hump h_c , with spacing 3.75 Å, indicative of the π - π interactions between disc cores, confirming the columnar nature of assembly. Therefore the structure of the assembly of **6.1** in the mesophase is columnar oblique (Col_{ob}).

Similarly, compound **6.2** found to exhibit columnar oblique phase in their mesophase region. Moreover, the calculated lattice parameters at temperature 25 °C at are found to be $a = 36.34 \text{ \AA}$, $b = 29.60 \text{ \AA}$ and $\alpha = 77.93^\circ$, details are given in the **Figure 2.6b & Table 2.3**.

Further, the compound **6.3** also show exhibit columnar oblique phase in their mesophase region. Moreover, the calculated lattice parameters at temperature 25 °C at are found to be $a = 44.12 \text{ \AA}$, $b = 39.53 \text{ \AA}$ and $\alpha = 69.84^\circ$, details are given in the **Figure 2.6c & Table 2.4**.

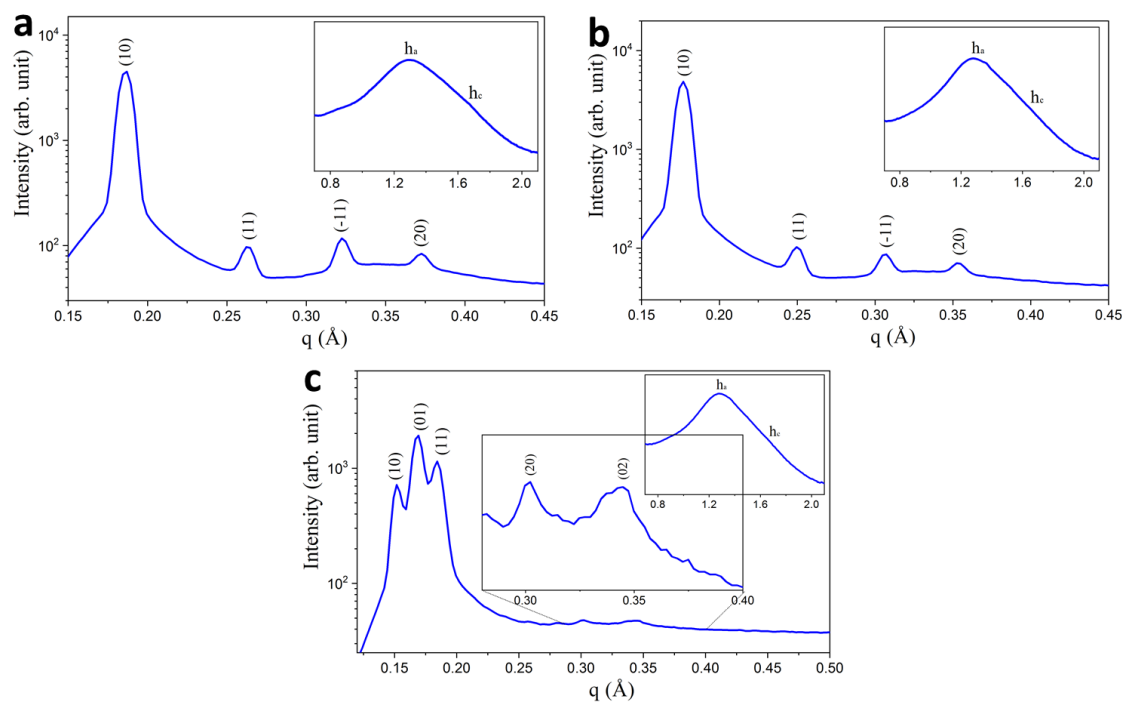


Figure 2.6: Small angle and wide angle (inset) x-ray diffraction pattern of compound (a) **6.1**, (b) **6.2** and (c) **6.3** at 25 °C.

TABLE 2.2: The observed and calculated d-spacings & planes of the diffraction peaks of **6.1** in oblique lattice observed at 25 °C. The lattice parameter are $a = 34.35$ Å, $b = 28.25$ Å and $\alpha = 78.19^\circ$.

(hk)	<i>d-spacing</i> <i>Experimental</i> d_{obs} (Å)	<i>d-spacing</i> <i>Calculated</i> d_{cal} (Å)	<i>Relative</i> <i>Intensity</i> $I(hk)$	<i>Multiplicity</i>	<i>Phase</i> $\Phi(hk)$
10	33.62	33.63	100.00	2	0
11	23.89	23.89	2.16	2	0
-11	19.49	19.49	2.60	2	0
20	16.87	16.81	1.87	2	π
h_a	4.84	Fluid alkyl chain			
h_c	3.75	π - π interaction			

TABLE 2.3: The observed and calculated d-spacings & planes of the diffraction peaks of 6.2 in oblique lattice observed at 25 °C. The lattice parameter are $a = 36.34 \text{ \AA}$, $b = 29.60 \text{ \AA}$ and $\alpha = 77.93^\circ$.

<i>(hk)</i>	<i>d-spacing Experimental</i> $d_{obs} (\text{\AA})$	<i>d-spacing Calculated</i> $d_{cal} (\text{\AA})$	<i>Relative Intensity</i> $I(hk)$	<i>Multiplicity</i>	<i>Phase</i> $\Phi(hk)$
10	35.54	35.54	100.00	2	0
11	25.17	25.17	2.13	2	0
-11	20.45	20.45	1.79	2	0
20	17.75	17.77	1.44	2	π
h_a	4.92	Fluid alkyl chain			
h_c	3.80	π - π interaction			

TABLE 2.4: The observed and calculated d-spacings & planes of the diffraction peaks of 6.3 in oblique lattice observed at 25 °C. The lattice parameter are $a = 44.12 \text{ \AA}$, $b = 39.53 \text{ \AA}$ and $\alpha = 69.84^\circ$.

<i>(hk)</i>	<i>d-spacing Experimental</i> $d_{obs} (\text{\AA})$	<i>d-spacing Calculated</i> $d_{cal} (\text{\AA})$	<i>Relative Intensity</i> $I(hk)$	<i>Multiplicity</i>	<i>Phase</i> $\Phi(hk)$
10	41.42	41.42	37.30	2	0
01	37.11	37.11	100.00	2	0
11	34.09	34.09	96.14	2	0
20	20.79	20.71	2.45	2	π
02	18.44	18.55	2.61	2	π
h_a	4.88	Fluid alkyl chain			
h_c	3.73	π - π interaction			

2.4 Photo-Physical Studies

2.4.1 Absorption and Emission Studies

This spectroscopic technique is a measure of diminishment of the intensity of light after passing through a material or solution. UV-Vis spectrum corresponds to energy levels and electronic excitation depending on the chemical bonds present in the substance to be

analysed. In case of UV-Vis spectrophotometry, the transitions that ensues in, occurring as a consequence of absorbing electro-magnetic radiation in UV-Vis region, are transitions happening in intra-molecular electronic energy states. Upon absorbing energy by a molecule, an electron is upgraded from an already filled molecular orbital to a vacant orbital with higher potential energy. The most probable electronic transition is to the lowest unoccupied molecular orbital (LUMO) from the highest occupied molecular orbital (HOMO).

The extent of light absorption rises up with the rise in the population of molecules capable of drawing the light of a specific wavelength in. Furthermore, the extent at which light is being absorbed is directly proportional to how well a molecule can absorb light in a specific wavelength. This gives rise to the Beer-Lambert's law, which asserts that at a given wavelength, the amount of absorption varies linearly with the sample concentration absorbing that wavelength and the length traversed by the light through that very sample which corresponds to the cell dimension.

$$A = \epsilon Cl$$

A = Measure of diminishment of intensity of the incident light i.e. Absorbance = $\log_{10}\left(\frac{I_0}{I}\right)$;
I₀ = intensity of the waves during irradiation; **I** = intensity of the radiation after attenuation; **l** = dimension of the cell containing sample (in centimetres); **c** = sample concentration, in mol/litre; **ε** = molar absorption coefficient ($M^{-1} \text{ cm}^{-1}$ where $M = \text{mol L}^{-1}$).²⁸

This technique cannot identify the unknown compound completely and exclusively. However, the use of very small quantities of the sample and rapid analysis of unknown compounds makes this a common routine analytical technique.

Fluorescence spectroscopy deals with the phenomenon called fluorescence occurring in a molecule which basically is a sort of luminescence originated due to excitation of a molecule by photons to an excited state. The emission spectrum provides information on qualitative as well as quantitative analysis which is a plot where emission is mapped against the wavelength for a known excitation.²⁹ After absorption of the given wavelength, a range of vibrational energy levels of the excited state gets occupied, resulting in relaxation to the lowest of the

vibrational levels (known as vibrational relaxation). This phenomenon where emission of light occurs due to the relaxation of the molecule to the singlet ground state from a singlet excited one, is known as Fluorescence and it lasts for a few nanoseconds.

Optical properties of all the TPN derivatives (**6.1-6.3**) were performed in solution phase in dichloromethane.³⁰ All the derivatives show similar crests in both of the absorption and emission spectra independent of the chains used as described in the **Table 2.5** and **Figure 2.7**. The most probable transition i.e. HOMO-LUMO transition is a primary transition and requires the wavelength (λ_{max}) of **357, 357** and **358 nm** for **6.1-6.3** which is in UV region (<380 nm).

Upon exciting the samples to the (λ_{max}) the emission spectra was recorded and all three of them emits at **428 nm** which expresses the fact that the emission is occurring in the **blue** region of the visible spectra.

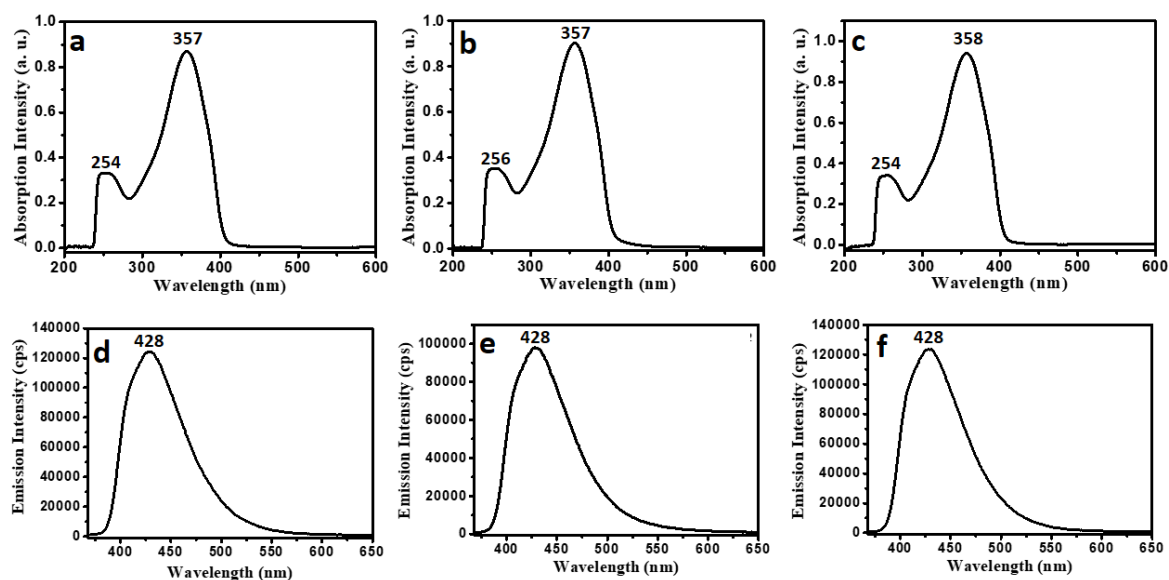


Figure 2.7: Photoluminescence spectra of the compounds **6.1-6.3**; (a)-(d) absorption and emission spectra of **6.1**; (b)-(e) absorption and emission spectra of **6.2**; (c)-(f) absorption and emission spectra of **6.3**.

TABLE 2.5: Summary of photoluminescence data

Compound	$\lambda_{\text{max, excitation}}$	$\lambda_{\text{max, emission}}$
6.1	357 nm	428 nm
6.2	357 nm	428 nm
6.3	358 nm	428 nm

2.4.2 Electrochemical Studies

As the name suggests, this process is a well-known and frequently performed electrochemical approach which is employed whenever redox processes are involved in a molecule. Here the potential of a working electrode is cycled and current originated is measured. The experimental setup for CV measurements includes a single chamber equipped with Ag/AgNO₃, platinum wire and glassy carbon are used as reference electrode, counter electrode and working electrode respectively.^{31,32} Thus by using this analytical technique one can measure E_{red} (reduction potential) and E_{ox} (oxidation potential).

For organic semiconductors, HOMO represents a band where oxidation process takes place which involves the energy essential for extracting an electron from a molecule to infinity, whereas LUMO represents a band where reduction process occurs which requires the proper energy to insert an electron to a molecule from infinity.³³ In this light, CV can be used to estimate not only the energy band gap (the HOMO-LUMO gap), but also the individual energy values of HOMO and LUMO of the organic compounds.³⁴

Cyclic voltammetry was performed on all the samples (**6.1-6.3**) which required milimolar solution, prepared by dissolving the respective compounds into HPLC DCM solution of TBAP (0.1M). The scanning was done at a rate of 50 mVs⁻¹. Tetrabutylammonium hexafluorophosphate or TBAP is used as a supporting electrolyte. The oxidation cycle onset and the reduction cycle onset were considered for the calculation of HOMO and LUMO levels (**Figure 2.8 & Table 2.6**).

$$E_{\text{HOMO}} = -(4.8 - E_{\frac{1}{2}, \text{Fc, Fc}^+} + E_{\text{oxd, onset}})$$

$$E_{LUMO} = -(4.8 - E_{\frac{1}{2},Fc,Fc^+} + E_{red,onset})$$

$$\Delta E_{g,CV} = E_{LUMO} - E_{HOMO}$$

Ferrocene (Fc) is used as a known as standard to calculate the energy of each of bands (i.e. HOMO and LUMO). The energy is supplied to the system in the form of potential which is applied externally through a source. When the reduction occurs, Fc^+ has to take electron from a cathode. But in order to make that possible, the energy of the electrons in the cathode has to have the energy which matches with the LUMO of Fc, which is achieved by increasing the potential difference itself. The force which drives this process is the difference in energy in between the electrode and the MO bands.

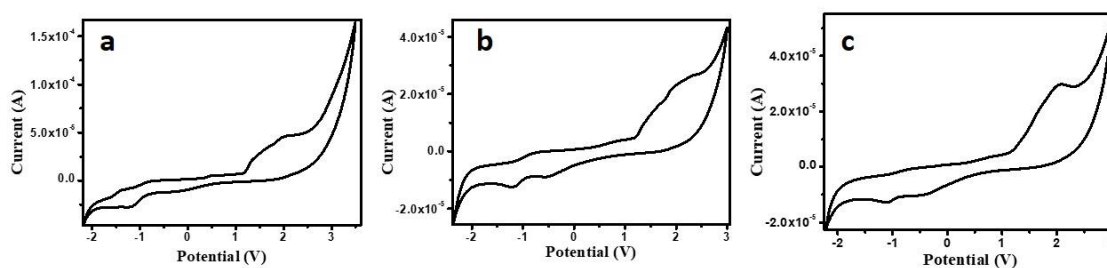


Figure 2.8: Cyclic voltammograms of (a) **6.1**, (b) **6.2** and (c) **6.3** in solution of TBAP (0.1 M) in HPLC DCM at a scanning rate 50 mVs^{-1} .

The band gap thus found can be correlated with the band gap that can be calculated from the Absorption Spectra. The following table summarizes the discussion.

Table 2.6: Comparing band gap from UV-Vis and CV of compound **6.1-6.3**.

Compound	λ_{max}	$\Delta E_{g,UV}$	E_{LUMO}	E_{HOMO}	$\Delta E_{g,CV}$
6.1	357 nm	3.47 eV	-3.44 eV	-5.48 eV	2.04 eV
6.2	357 nm	3.47 eV	-3.42 eV	-5.49 eV	2.07 eV
6.3	358 nm	3.46 eV	-3.43 eV	-5.47 eV	2.04 eV

2.4.3 OLED Device Fabrication

As all the compounds are showing very good emissive property, we have fabricated the OLEDs based on compound **6.1** in order to see their electroluminescence (EL) behaviour and device performance. The devices were fabricated in the structure of ITO/PEDOT:PSS/compound **6.1** doped in CBP/TPBi/LiF/Al, as shown in **Figure 2.9a**. We have used four different wt% of emitter (**6.1**) i.e. 1 wt%, 3 wt%, 5 wt% and 100 wt%. Upon variation of emitter (**6.1**) wt% it is observed that at 3 wt% it exhibited best device performance with EQE of 3.7% showing deep-blue colour emission having (CIE) coordinate (0.16, 0.12) (**Figure 2.9**). The summary of all the device performances were listed in **Table 2.7**.

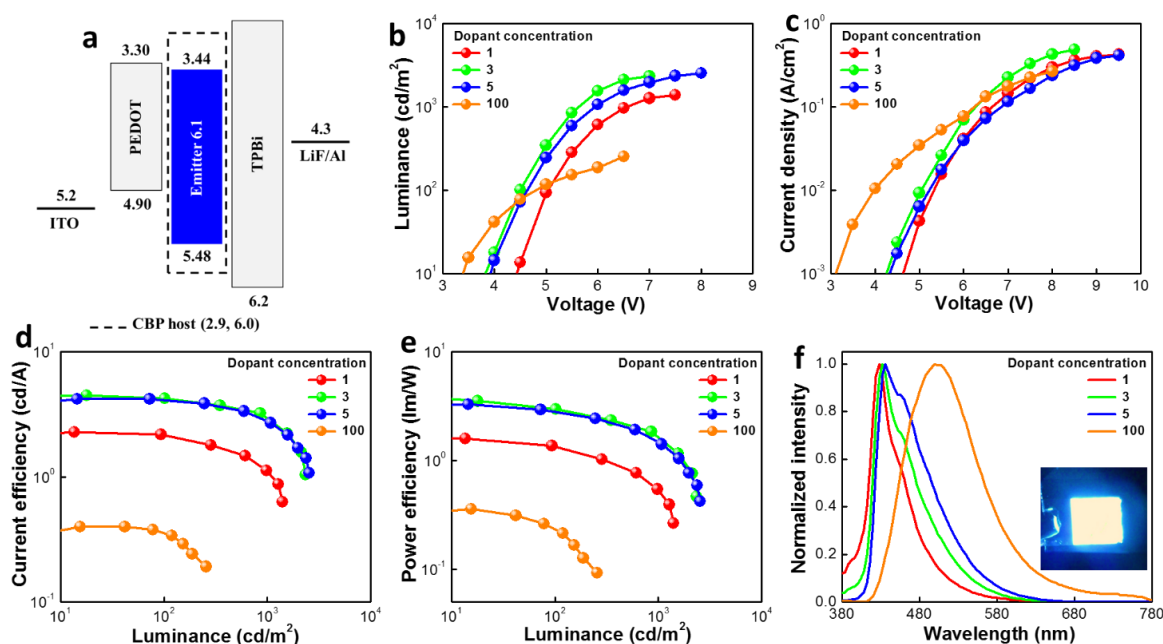


Figure 2.9: (a) Diagram of energy-level of emitter **6.1** used with (CBP) host for fabrication of the device. (b) luminance-voltage, (c) Current density-voltage, (d) current efficiency-luminance, (e) power efficiency-luminance and (f) electroluminescence plots of the solution-processed OLED devices using CBP host with 1, 3, 5 and 100 wt% **6.1** dopant concentrations. Inset of (f) shows EL emission of the OLED device. (OLED device fabrication studies were performed in collaboration with Prof. J.H. Jou and his team from NTHU, Taiwan).

Table 2.7: Effect of doping concentration on the power efficiency (PE), current efficiency (CE), external quantum efficiency (EQE), CIE coordinates, and maximum luminance of solution-processed OLED devices with the CBP host for **6.1**.

Dopant Conc. (wt%)	Turn-on Voltage (V)	PE _{max} / CE _{max} / EQE _{max} (lm W ⁻¹ / cd A ⁻¹ / %)	PE ₁₀₀ / CE ₁₀₀ / EQE ₁₀₀ (lm W ⁻¹ / cd A ⁻¹ / %)	CIE coordinates	Max. Lum. (cd m ⁻²)
1	4.5	1.6/2.3/3.2	1.4/2.2/3.2	(0.16, 0.08)	1403
3	4.1	3.7/4.0/3.7	2.7/3.9/3.7	(0.16, 0.12)	2424
5	4.1	3.0/4.2/3.2	2.9/4.1/3.2	(0.16, 0.16)	2564
100	3.6	1.7/2.4/0.2	1.4/2.3/0.1	(0.24, 0.41)	256

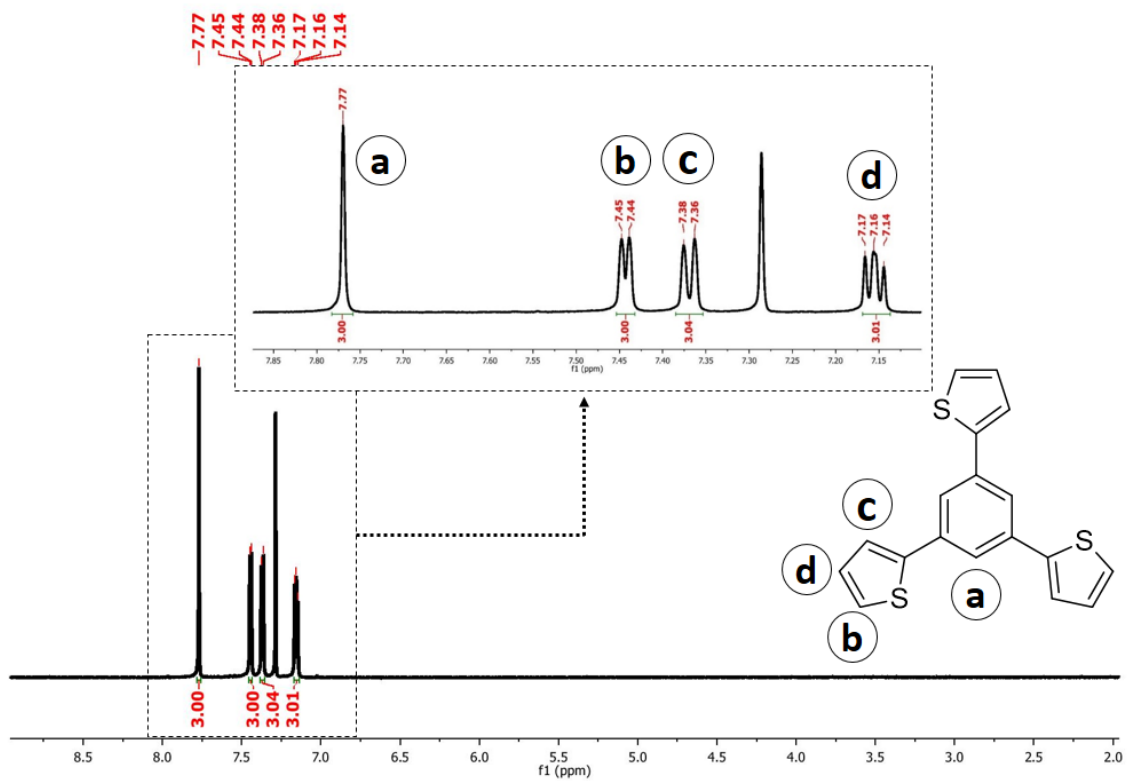
Chapter 3

CONCLUSION

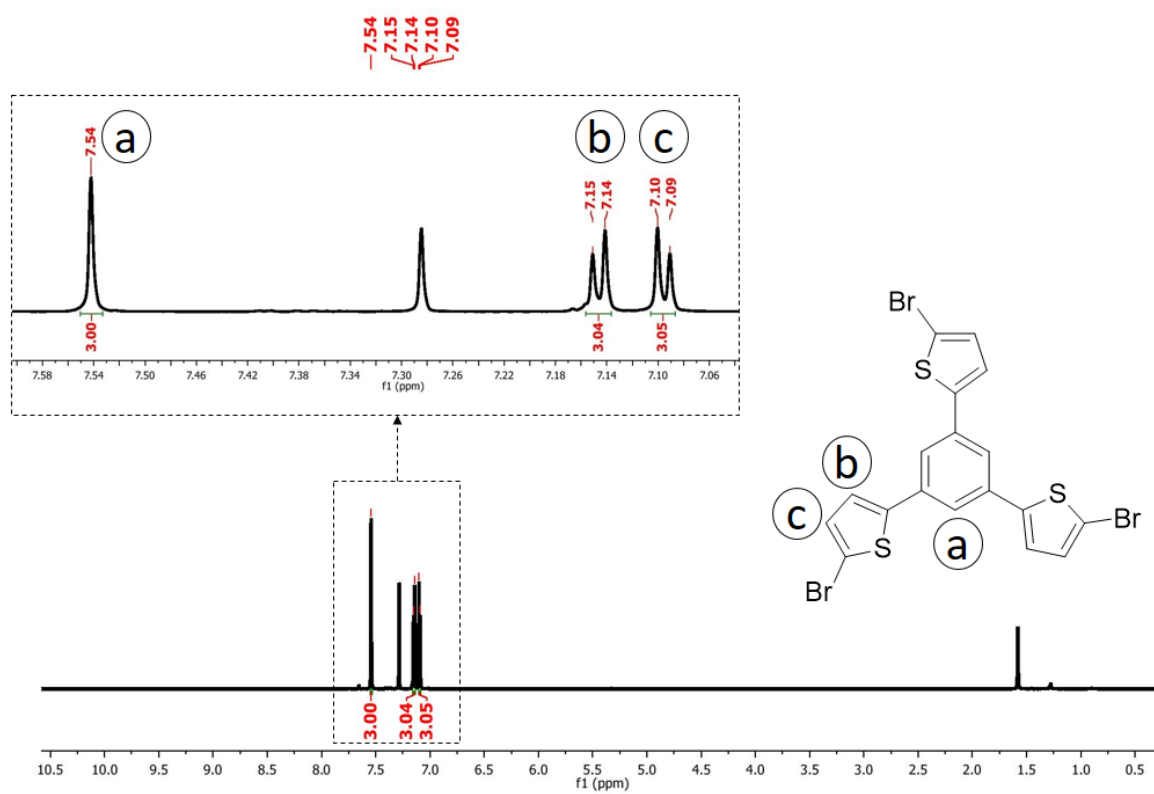
We have thus successfully synthesized all the derivatives of TPN series, which show DLC properties especially exhibiting blue luminescence. Characterization of all of the samples were brought to fruition by NMR, DSC, XRD, POM and TGA. Photo-physical studies were performed using UV-Vis spectroscopy, fluorescence and electrochemical characterization was done by cyclic voltammetry studies. The samples showed blue luminescence when irradiated in UV chamber, which opens up a new possibility as a potential material in OLED devices.

APPENDICES

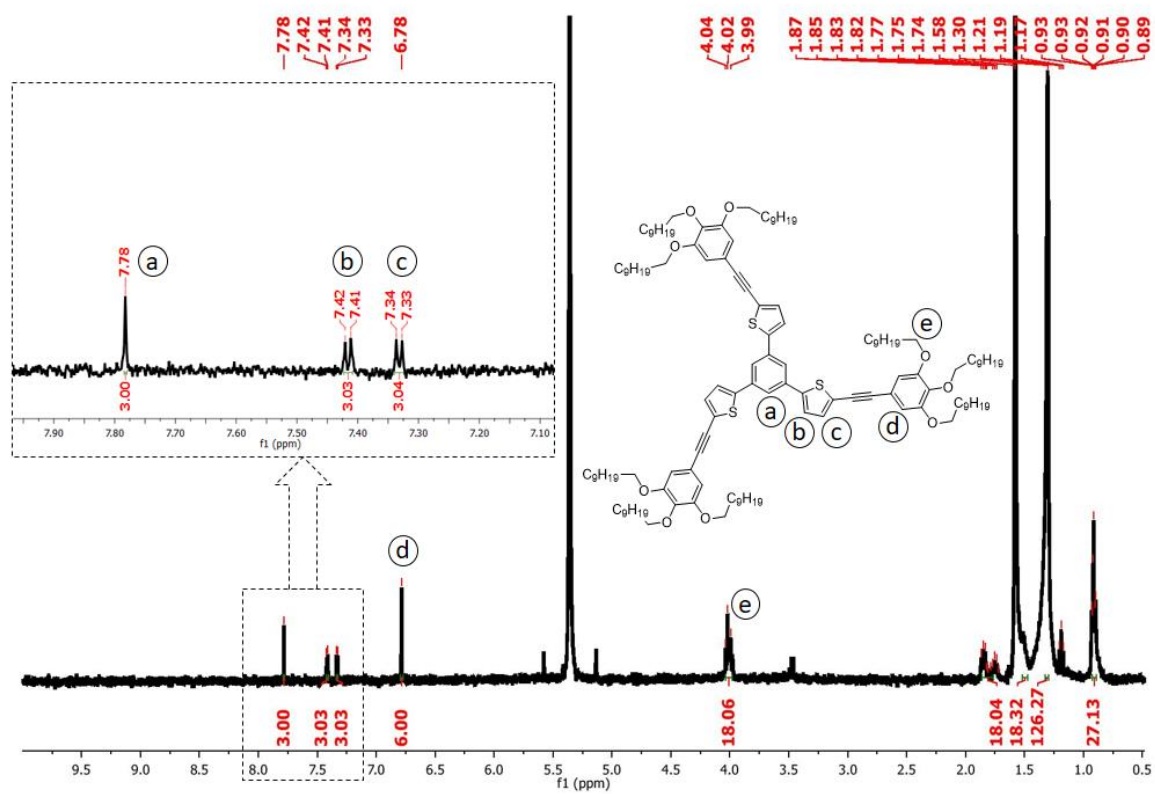
1. ^1H NMR of compound **1**



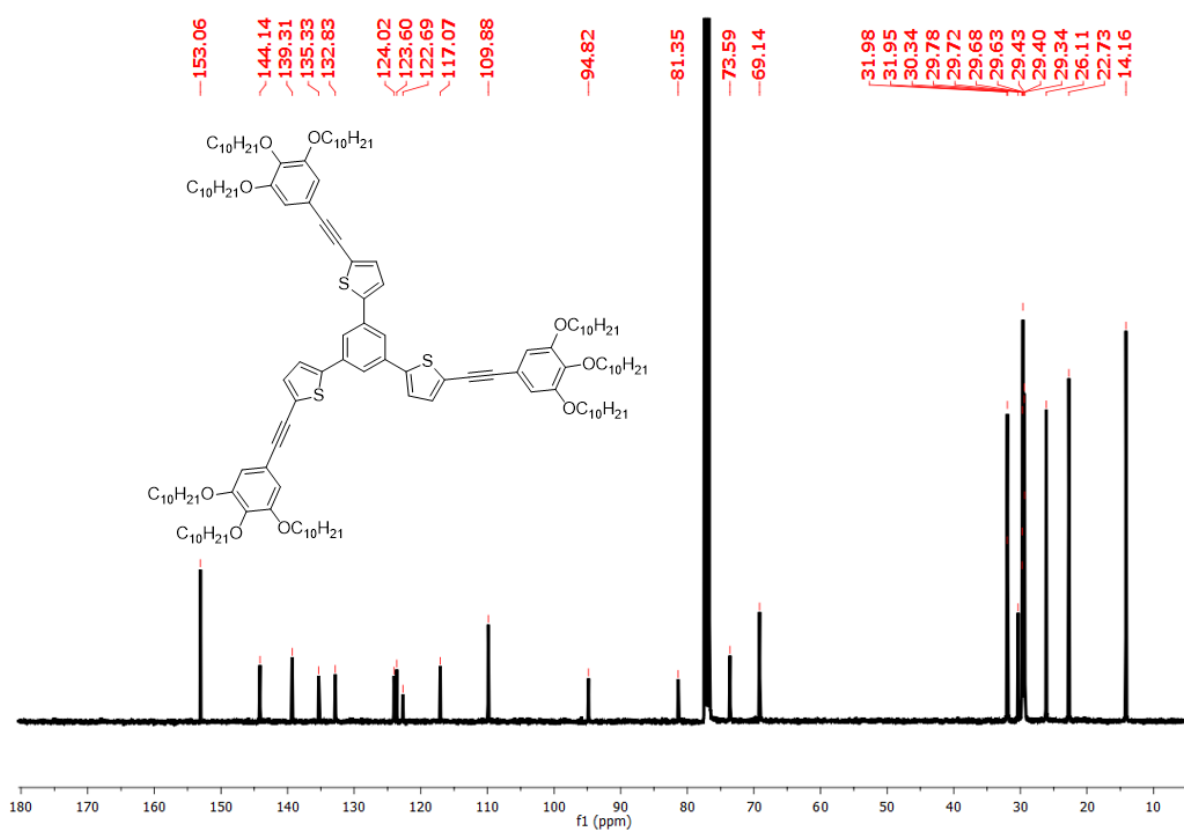
2. ^1H NMR of compound 2



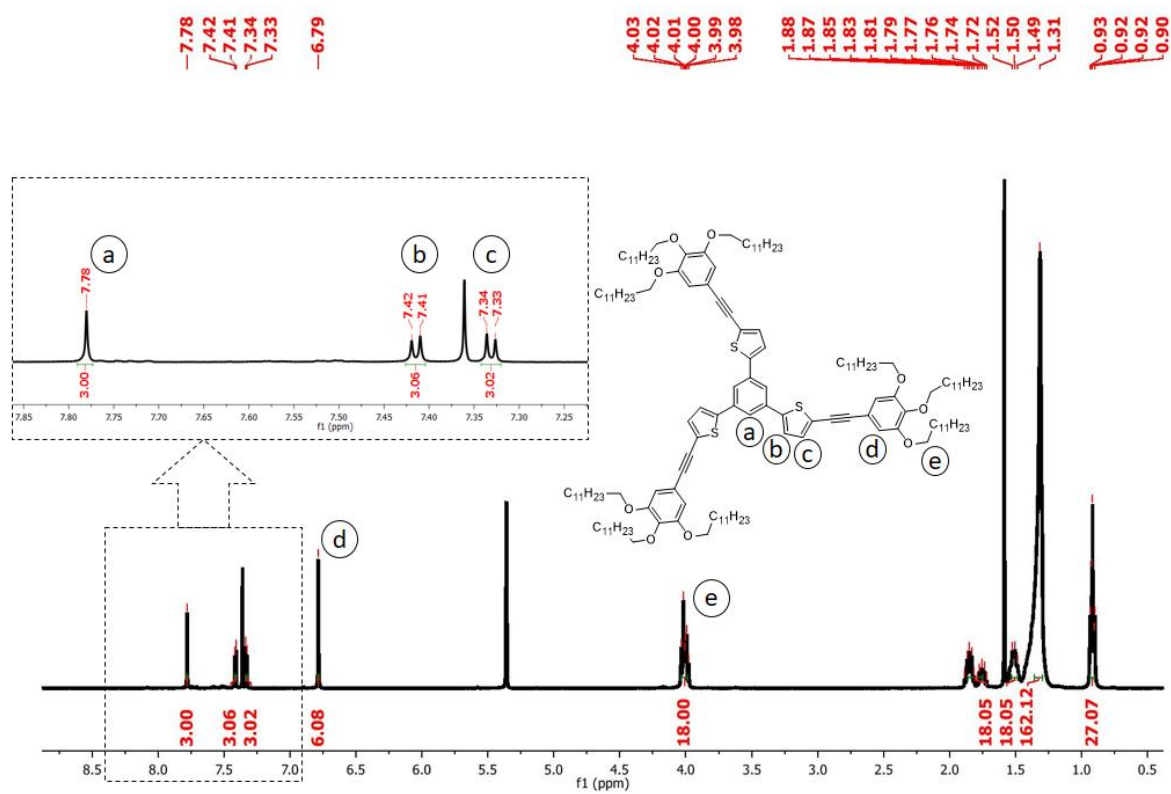
3. ^1H NMR of compound **6.1**



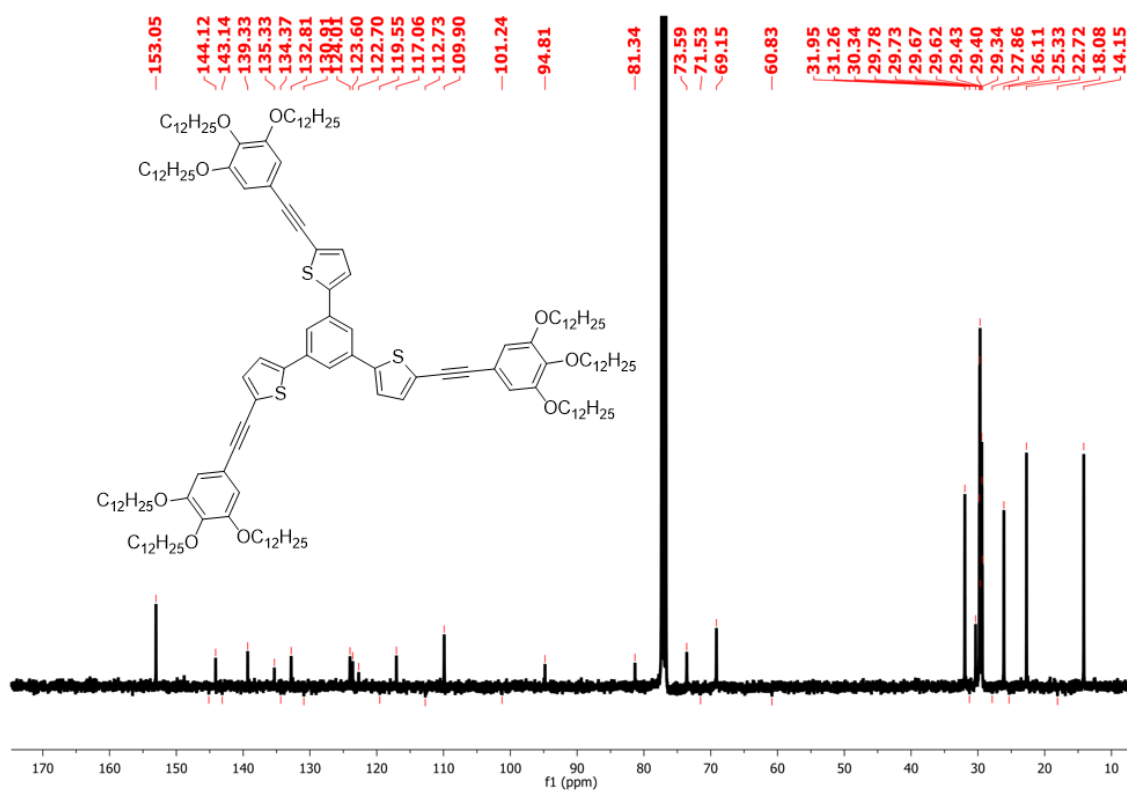
^{13}C NMR of Compound **6.1**



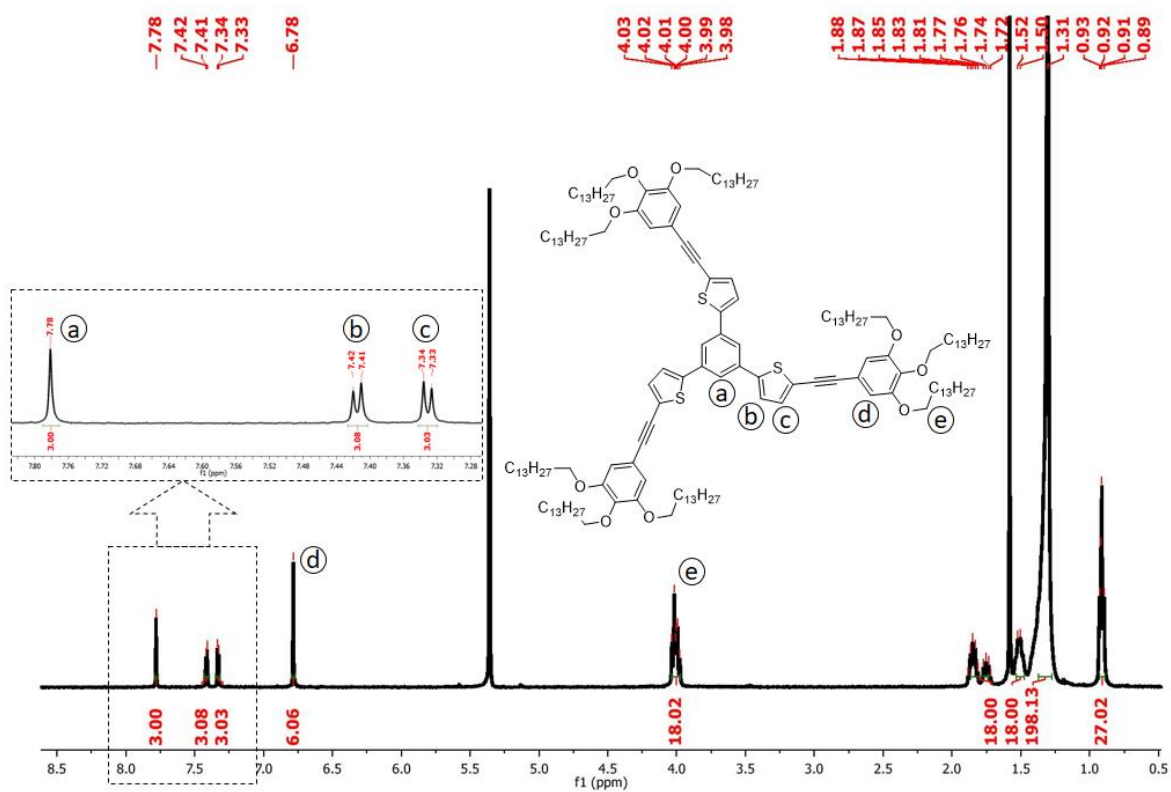
4. ^1H NMR of compound **6.2**



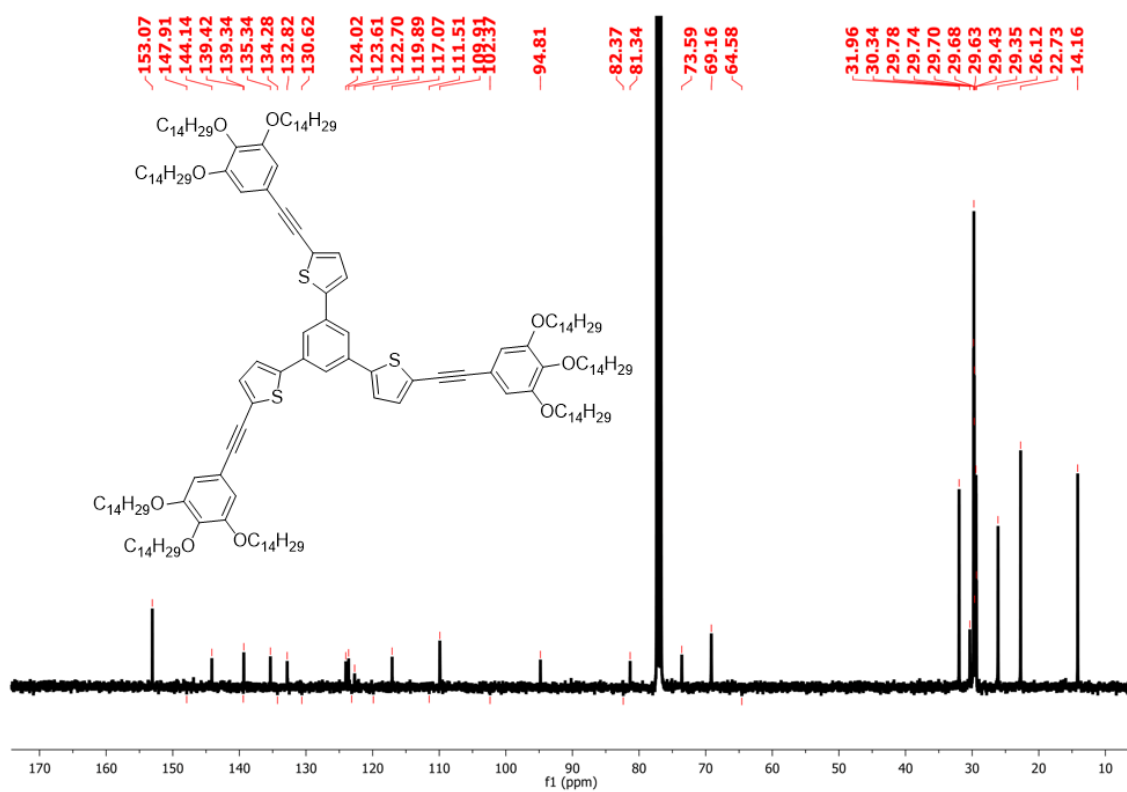
^{13}C NMR of the compound **6.2**



5. ^1H NMR of compound **6.3**



^{13}C NMR of the compound **6.3**



BIBLIOGRAPHY

1. Collings, P. J. Liquid Crystals: Nature's Delicate Phase of Matter; *Princeton University Press*: **2002**.
2. March, N. H.; Tosi, M. P. Introduction to Liquid State Physics; *World Scientific*: **2002**.
3. Kumar, S. Chemistry of Discotic Liquid Crystals: from Monomers to Polymers. *CRC Press*: **2010**.
4. Chandrasekhar, S. Liquid Crystals, 2nd ed. *Cambridge University Press*: **1992**.
5. Andrienko, D. Introduction to Liquid Crystals. *J. Mol.* **2018**, *267*, 520-541.
6. Goodby, J.; Görtz, V.; Cowling, S.; Mackenzie, G.; Martin, P.; Plusquellec, D.; Benvegnu, T.; Boullanger, P.; Lafont, D.; Queneau, Y., et al. Thermotropic Liquid Crystalline Glycolipids. *Chem. Soc. Rev.* **2007**, *36*, 1971-2032.
7. Chandrasekhar, S.; Sadashiva, B.; Suresh, K. Liquid Crystals of Disc-Like Molecules. *Pramana* **1977**, *9*, 471-480.
8. Simpson, C. D.; Wu, J.; Watson, M. D.; Müllen, K. From Graphite Molecules to Columnar Superstructures—An Exercise in Nanoscience. *J. Mater. Chem.* **2004**, *14*, 494-504.
9. Ichihara, M.; Suzuki, H.; Mohr, B.; Ohta, K. Different Disc Structures in the Hexagonal Columnar Mesophases of 2, 3-Dicyano-6,7,10,11-tetraalkoxy-1,4-diazatriphenylenes and 2,3-dicyano-6,7,10,11-tetraalkoxytriphenylenes. *Liq. Cryst.* **2007**, *34*, 401-410.
10. Kato, T.; Yasuda, T.; Kamikawa, Y.; Yoshio, M. Self-Assembly of Functional Columnar Liquid Crystals. *Chem. Commun.* **2009**, 729-739.
11. Kumar, S. Self-Organization of Disc-Like Molecules: Chemical Aspects. *Chem. Soc. Rev.* **2006**, *35*, 83-109.
12. Bisoyi, H. K.; Kumar, S. Discotic Nematic Liquid Crystals: Science and Technology. *Chem. Soc. Rev.* **2010**, *39*, 264-285.
13. Tang, C. W.; VanSlyke, S. A. Organic Electroluminescent Diodes. *Appl. Phys. Lett.* **1987**, *51*, 913-915.
14. Clark, N. A.; Lagerwall, S. T. Sub Microsecond Bi-Stable Electro-Optic Switching in Liquid Crystals. *Appl. Phys. Lett.* **1980**, *36*, 899-901.
15. Müllen, K.; Scherf, U. Organic Light Emitting Devices: Synthesis, Properties and Applications. *JWS*: **2006**.
16. Zhang, S.; Guo, Y.; Wang, L.; Li, Q.; Zheng, K.; Zhan, X.; Liu, Y.; Liu, R.; Wan, L. J. Synthesis, Self-Assembly and Solution-Processed Field-Effect Transistors of a Liquid Crystalline Bis(dithienothiophene) Derivative. *J. Phys. Chem. C* **2009**, *113*, 16232-16237.
17. Dyer, A. L.; Thompson, E. J.; Reynolds, J. R. Completing the Color Palette with Spray-Processable Polymer Electrochromics. *ACS Appl. Mater. Inter.* **2011**, *3*, 1787-1795.

18. Schulze, B. M.; Watkins, D. L.; Zhang, J.; Ghiviriga, I.; Castellano, R. K. Estimating the Shape and Size of Supramolecular Assemblies by Variable Temperature Diffusion Ordered Spectroscopy. *Org. Biomol. Chem.* **2014**, *12*, 7932-7936.
19. Kotha, S.; Todeti, S.; Bala Gopal, M.; Datta, A. Synthesis and Photophysical Properties of C3-Symmetric Star-Shaped Molecules Containing Heterocycles Such as Furan, Thiophene and Oxazole. *ACS Omega* **2017**, *2*, 6291-6297.
20. Kayal, H. S. Design and synthesis of novel discotic liquid crystals. *Electronic Theses and Dissertations.* **2012**, 4819.
21. Wöhrle, T.; Wurzbach, I.; Kirres, J.; Kostidou, A.; Kapernaum, N.; Litterscheidt, J.; Haenle, J. C.; Staffeld, P.; Baro, A.; Giesselmann, F.; Laschat, S. Discotic Liquid Crystals. *Chem. Rev.* **2016**, *116*, 1139-1241.
22. De, J.; Bala, I.; Gupta, S. P.; Pandey, U. K.; Pal, S. K. High Hole Mobility and Efficient Ambipolar Charge Transport in Heterocoronene-Based Ordered Columnar Discotics. *J. Am. Chem. Soc.* **2019**, *141*, 18799-18805.
23. Dierking, I. Textures of Liquid Crystals. *John Wiley & Sons:* **2003**.
24. Groenewoud, W. M. Characterisation of Polymers by Thermal Analysis. *Elsevier:* **2001**, *Chapter 1*, 10-60.
25. Pecharsky, V.; Zavalij, P. Fundamentals of Powder Diffraction and Structural Characterization of Materials. *Springer Science & Business Media SSBM:* **2008**.
26. Chatterjee, S. K. Crystallography and the World of Symmetry. *SSBM:* **2008** *Vol. 113*.
27. Prasad, S. K.; Rao, D. S.; Chandrasekhar, S.; Kumar, S. X-Ray Studies on the Columnar Structures of Discotic Liquid Crystals. *Mol. Cryst. Liq. Cryst.* **2003**, *396*, 121-139.
28. Skoog, D. A.; Crouch, S. A.; Holler, F. J. Principles of Instrumental Analysis. *Belmont, CA: Thompson Brooks/Cole:* **2007**, *6th Edition*
29. Giovanella, U.; Pasini, M.; Botta, C. In Applied Photochemistry. *Springer:* **2016**, 145-196.
30. Kaafarani, B. R. Discotic liquid crystals for opto-electronic applications. *Chem. Mater.* **2010**, *23*, 378-396.
31. De, J.; Yang, W.-Y.; Bala, I.; Gupta, S. P.; Yadav, R. A. K.; Dubey, D. K.; Chowdhury, A.; Jou, J.-H.; Pal, S. K. Room-Temperature Columnar Liquid Crystals as Efficient Pure Deep Blue Emitters in Organic Light-Emitting Diodes with an External Quantum Efficiency of 4.0%. *ACS Appl. Mater. Interfaces* **2019**, *11*, 8291-8300.
32. Pope, M.; Swenberg, C. E. Electronic Processes in Organic Crystals and Polymers. *OUP-USA:* **1999**.
33. Van de Craats, A. M.; Warman, J. M. The Core-Size Effect on the Mobility of Charge in Discotic Liquid Crystalline Materials. *Adv. Mater.* **2001**, *13*, 130-133.

34. Setia, S.; Sidiq, S.; De, J.; Pani, I.; Pal, S. K. Applications of Liquid Crystals in Biosensing and Organic Light-emitting Devices: Future Aspects. *Liq. Cryst.* **2016**, *43*, 2009-2050.

